A PROBABILISTIC DEFORMATION DEMAND MODEL AND FRAGILITY

ESTIMATES FOR ASYMMETRIC OFFSHORE JACKET PLATFORMS

A Thesis

by

MICHAEL BROOKS FALLON

Submitted to the Office of Graduate Studies of
Texas A&M University
in partial fulfillment of the requirements for the degree of

MASTER OF SCIENCE

Approved by:

Co-Chairs of Committee,   Paolo Gardoni
    Luciana Barroso
Committee Member,   Colleen Murphy
Head of Department,   John Niedzwecki

December 2012

Major Subject: Civil Engineering

ABSTRACT

Interest in evaluating the performance and safety of offshore oil and gas platforms has been expanding due to the growing world energy supply and recent offshore catastrophes. In order to accurately assess the reliability of an offshore platform, all relevant uncertainties must be properly accounted for. This necessitates the development of a probabilistic demand model that accounts for the relevant uncertainties and model errors.

In this study, a probabilistic demand model is developed to assess the deformation demand on asymmetric offshore jacket platforms subject to wave and current loadings. The probabilistic model is constructed by adding correction terms and a model error to an existing deterministic deformation demand model. The correction terms are developed to capture the bias inherent in the deterministic model. The model error is developed to capture the accuracy of the model. The correction terms and model errors are estimated through a Bayesian approach using simulation data obtained from detailed dynamic analyses of a set of representative asymmetric offshore platform configurations. The proposed demand model provides accurate and unbiased estimates of the deformation demand on offshore jacket platforms.

The developed probabilistic demand model is then used to assess the reliability of a typical offshore platform considering serviceability and ultimate performance levels. In addition, a sensitivity analysis is conducted to assess the effect of key parameters on the results of the analyses. The proposed demand model can be used to assess the

reliability of different design options and for the reliability-based optimal design of offshore jacket platforms.

DEDICATION

To my family and friends

ACKNOWLEDGEMENTS

I would like to thank my committee chair, Dr. Gardoni, for his time, guidance, and support throughout the course of this research. I would also like to thank my colleague, Maryam Mardfekri, for the time she took to guide me through this research.

Thanks also go to my friends and colleagues for making my time at Texas A&M University an unforgettable experience.

Finally, thanks to my mother and father for their inspiration and encouragement over the course of my education, and especially during this final stages of this research project.

NOMENCLATURE

x	Vector of structural properties
w	Vector of loading parameters
GC	Geometric center
CM	Center of mass
CR	Center of rigidity
σ	Standard deviation
COV	Coefficient of variation
h	Height of offshore platform
d	Water depth
c	Clearance between MSL and platform deck
H	Wave height
T	Wave period
ω	Wave frequency
v	Current velocity
m	Platform mass
L	Platform deck length
X_r	CR x-coordinate
Y_r	CR y-coordinate
X_m	CM x-coordinate
Y_m	CM y-coordinate

K_x	Lateral stiffness
K_θ	Torsional stiffness
n	Number of platform legs
D	Diameter of platform legs
R	Distance from CR
r	Distance between CM and CR (eccentricity)
ω_n	Natural frequency of platform
$\omega_{\theta n}$	Natural torsional frequency of platform
α, β	Raleigh damping coefficients
C_D	Drag coefficient
C_m	Added mass coefficient
C_M	Inertia coefficient
ρ	Density of seawater

TABLE OF CONTENTS

Page

LIST OF FIGURES

Page

LIST OF TABLES

1. INTRODUCTION

1.1 Background

Offshore oil and gas projects are responsible for nearly one third of the world's energy supply. As this fraction continues to increase, as well as the world energy demand, oil and gas production has to move towards more hostile offshore environments. Because of the growing importance of offshore oil and gas, technical analysis and design of offshore platforms has become an important field in engineering (Xiaoyu and Hongnan 2010). In addition, the recent failure of the Deepwater Horizon drilling rig in April of 2010 that killed 11 people, injured several others, and caused a massive environmental crisis illustrated the importance of safe and reliable offshore structures (Skogdalen et al. 2012). Presently, there are thousands of offshore platforms in use, and their structural safety and reliability are more important than ever.

The *cost of energy* is critical to the success of an offshore petroleum production project. In the case of offshore drilling platforms, the cost of energy is the cost of design, construction, installation, maintenance and repair, and operation. A reliability analysis of offshore structures can decrease the need for costly repair, maintenance, and downtime. In addition, reliability-based design of an offshore platform can prevent overly conservative designs that increase the cost of the project. Therefore, reliability-based designs of offshore platforms provide an optimal use of resources for hydrocarbon production. Accordingly, a framework is needed for the assessment of the structural reliability of offshore platforms.

Offshore platforms can be broadly categorized into two groups based on the existence or not of a support structure: fixed platforms and floating platforms. Fixed platforms are bottom supported structures that extend to the seabed, while floating platforms are structures that float near the water surface and are not structurally connected to the seabed. The main advantage of floating type offshore platforms is the water depths in which they can be installed. There is no structural constraint with regards to the depth of water in which these platforms can operate because there is no structural system that extends to the seafloor. However, floating platforms typically have greater stability and dynamics problems due to the lack of a support structure. Fixed platforms are typically installed in more shallow waters up to approximately 520 meters. The main advantages of these platforms are their relative stability and limited movement due to the presence of a support structure attached to the seabed. However, it is not economical to build the support structures in deep waters. Because of their wide use and importance, this study focuses on fixed offshore platforms.

Fixed offshore platforms can be categorized into three types: steel jacket platforms, concrete gravity platforms, and compliant towers. Jacket platforms are supported by a framed structure with pile foundations. Concrete gravity platforms are supported by massive concrete structures that remain in place on the seabed without the need for piles. Compliant towers are very similar to jacket platforms but are installed in deeper waters, and therefore are much narrower and designed to be more flexible. Steel jackets are the most common fixed offshore platforms. Thus, we will evaluate this type of platform within the scope of this study.

Several studies have been carried out to assess the structural reliability of offshore platforms subject to environmental loading. Jensen et al. (1991) studied the reliability of offshore platforms against overturning, an ultimate limit state. They showed that the sea state does have a large influence on the overturning moment. Nadim and Gudmestad (1994) studied the reliability of a particular oil field in the North Sea under earthquake loads. Kirkegaard et al. (1991) considered the fatigue reliability of an offshore mono tower platform, and Karamchandani et al. (1991) examined combined fatigue and extreme loading reliability of offshore platforms. Both of these studies considered component and system failure which are ultimate limit states. However, there are some limitations to these studies. First, none of them consider the mass and/or rigidity eccentricity and the resulting torsional behavior in typical offshore jacket platforms. The asymmetry of offshore platforms is often inevitable due to many factors, including asymmetric structure plan and accidental mass and rigidity eccentricity, and therefore, the asymmetry of the offshore structures should be considered. Furthermore, these available approaches are limited to the ultimate failure modes of the offshore platform, and do not consider serviceability limit states, typically governed by the displacement of the platform.

As offshore platforms are being installed in deeper waters, the dynamic response of offshore platforms due to wave and current action has become the focus of many researchers (Hahn 1992; Bea et al. 1999). Computational modeling is being widely used to determine the demand on the structural components of offshore platforms. These analyses require accurate modeling of the dynamic response of the structure and

evaluation of the environmental loading including wave and current loading. Nataraja and Kirk (1977) developed the equation of motion for a gravity platform under wave forces and studied the dynamic responses. Xiaoyu and Hongnan (2010) similarly evaluated the dynamic response of offshore platforms, but also considered the inherent asymmetry of the structure and corresponding torsional response. However, Xiaoyu and Hongnan did not assess the effects of the torsional behavior on the reliability of offshore platforms.

This study addresses the limitations listed above. It incorporates the dynamic response of asymmetric offshore platforms into a reliability framework. The dynamic response formulation follows Xiaoyu and Hongnan (2010) to consider the asymmetry of offshore platforms which results in more realistic analyses. Finally, the formulation of the reliability framework can consider both serviceability and ultimate limit states. The drift of the drill pipe and the drift of the structural legs of the platform are studied. The drill pipe drift corresponds to a serviceability limit state, as large displacements of the drill pipe will suspend oil or gas production operations on the platform. On the other hand, the platform leg drift is considered an ultimate limit state, as large displacements of these structural members can result in structural failure. Including serviceability in the proposed framework ensures that the day to day operation of an offshore platform, and not just ultimate failure, is considered.

This thesis presents the formulation of a probabilistic demand model for asymmetric offshore jacket platforms that accounts for the prevailing uncertainties. This is done by developing corrections terms that correct the inherent bias and uncertainty in

existing deterministic demand models. Next, fragility estimates are presented for example asymmetric offshore jacket platforms. The probabilistic demand models are used to compute the fragility of the structure with respect to a deformation failure mode.

The reliability framework developed in this study can potentially lead to significant decreases in the cost of energy for asymmetric offshore jacket platforms based on accurate estimates of their reliability. Furthermore, the results of this study will be of interest to the civil, ocean, and petroleum engineering communities.

1.2   Research Objectives

The goal of this thesis is to develop a reliability framework for asymmetric platforms that accounts for the prevailing uncertainties, including model errors, measurement errors and statistical uncertainty. To achieve this overall goal, this study has two objectives:

Objective 1: Develop a probabilistic deformation demand model for asymmetric offshore platforms. A demand model is a mathematical expression that relates the structural demand of interest (e.g. drift of the drill pipe or drift of the platforms legs) to the environmental loading and system properties. As opposed to developing new models, the probabilistic deformation demand model is formulated by adding correction terms to an existing deterministic demand model following a general formulation developed by Gardoni et al. (2002). This framework corrects the bias in the deterministic model and accounts for the inherent uncertainties.

Objective 2: Develop fragility estimates for example asymmetric offshore platforms. An evident application of the probabilistic demand model is to estimate the structural fragility of a given asymmetric offshore platform. Fragility is defined as the probability of failure for a given set of demand variables. Predictive fragility estimates are used to develop fragility curves for example offshore platforms.

1.3   Organization of Thesis

This thesis is organized using a section-subsection format. There are four sections and within each section there are subsections. The word "section" corresponds to the first heading level and "subsection" corresponds to the second and above heading levels. Descriptions for each section in this thesis are listed below.

- Section 1 (current section) gives an introduction and background information of this thesis, including the project description, the current state of knowledge on the subject, and the project's significance. Next, the overall goal and objectives are given, followed by the organization of this thesis.

- Section 2 develops the probabilistic deformation demand model for asymmetric offshore platforms. This section gives an overview of the platform system considered, and then describes the deterministic model selected for use in this study. Next, the experimental method and data are discussed, and the model selection process is outlined.

- Section 3 uses the proposed probabilistic deformation demand model to estimate the fragility of an example offshore platform. The analysis is conducted

considering a serviceability limit state and an ultimate limit state. In addition, a sensitivity analysis of selected variables is carried out.

- Section 4 discusses conclusions of this thesis and proposes future work that could further the results of this study.

2. PROBABILISTIC DEMAND MODEL

2.1   Introduction

This section develops a probabilistic deformation demand model for asymmetric offshore jacket platforms. A demand model is an analytical expression or procedure that relates the demand on a structural component to the properties of the system considered (e.g. material properties, structural dimensions, and boundary conditions) and environmental loading. The main purpose of a structural demand model is to predict the structural demand quantities of interest for given system and loading properties. A probabilistic demand model accounts for the uncertainties inherent in predicting the demand of interest. These uncertainties can be categorized into two broad types, as described by Gardoni et al. (2002): aleatory uncertainties and epistemic uncertainties. Aleatory uncertainties are inherent in nature and cannot be influenced by the observer, while epistemic uncertainties are a result of our lack of knowledge, our deliberate choice to simplify matters, errors in measurements and observations, and the finite size of observation samples. Although aleatory uncertainties are inevitable and cannot be reduced, epistemic uncertainties can be reduced by use of an improved demand model. Ideally, a probabilistic demand model should be derived from first principles (e.g. the rules of mechanics) and incorporate experimental and field data when available. Rather than creating a new model, we develop the probabilistic demand model by adopting an existing deterministic demand model or analysis procedure and add correction terms to capture potential bias in the deterministic model, as outlined in Gardoni et al. (2002,

8

2003). An offshore jacket platform is subject to demands that could lead to failure in a serviceability or ultimate limit state due to excessive deformations. Following Gardoni et al. (2002, 2003), the proposed demand model for given material properties, structural dimensions, and boundary conditions, x, and also for given external loading, including wave and current loadings, w, can be formulated as

$$D_k(x, w, \Theta_{D,k}) = \hat{d}_k(x, w) + \gamma_{D,k}(x, w, \theta_{D,k}) + \sigma_{D,k}\varepsilon_{D,k} \qquad (2.1)$$

where $\Theta_{D,k} = (\theta_{D,k}, \sigma_{D,k})$, $\theta_{D,k}$ = vector of unknown model parameters, $\hat{d}_k(x, w)$ = selected deterministic demand model, $\gamma_{D,k}(x, w, \theta_{D,k})$ = correction term for the bias inherent in the deterministic model, $\sigma_{D,k}\varepsilon_{D,k}$ = model error, $\varepsilon_{D,k}$ = random variable with zero mean and unit variance, and $\sigma_{D,k}$ = unknown standard deviation of the model error. Note that for given x, $\theta_{D,k}$, and $\sigma_{D,k}$ we have $Var[D_k(x, w, \Theta_{D,k})] = \sigma_{D,k}^2$ as the variance of the model. The index k indicates the considered mode of failure, and a different deterministic demand model will be used for each failure mode. Within the scope of this project, the only demand of interest is the deformation demand on the structure. Therefore, $k = \delta$ for the deformation demand. In writing Eq. (2.1), two assumptions need to be satisfied: (1) the model variance is constant (homoscedasticity assumption), and (2) $\varepsilon_{D,k}$ follows the normal distribution (normality assumption). To satisfy these assumptions, a variance stabilizing transformation of the demand quantities is typically used (Box and Cox 1964). In this study, a logarithmic transformation is used to satisfy the above assumptions. That is, $D_\delta = ln(\Delta/h)$, where Δ = deformation demand and h = height of the offshore platform; $\hat{d}_\delta = ln(\hat{\Delta}/h)$ where $\hat{\Delta}$ is the deterministic

9

estimate of the deformation demand. The quantity Δ/h is defined as the "drift" of the platform.

The correction term, $\gamma_{D,k}$, is added to correct the bias and account for the missing terms in the deterministic model. Following Gardoni et al. (2002), this correction term will be calculated as

$$\gamma_{D,k}(\boldsymbol{x},\boldsymbol{w},\boldsymbol{\theta}_{D,k}) = \sum_{i=1}^{p} \theta_{D,ki}h_{ki}(\boldsymbol{x},\boldsymbol{w}) \tag{2.2}$$

where $\boldsymbol{\theta}_{D,k} = [\theta_{D,ki}]$, and $h_{ki}(\boldsymbol{x},\boldsymbol{w})$ = candidate explanatory functions that might be significant in correcting $\hat{d}_k(\boldsymbol{x},\boldsymbol{w})$, and p = the number of explanatory basis functions. The model parameters, $\boldsymbol{\Theta}_{D,k} = (\boldsymbol{\theta}_{D,k},\sigma_{D,k})$, can be estimated following a Bayesian approach using field, laboratory, and/or virtual (simulated) data (Box and Tiao 1992). By examining the posterior statistics of the unknown parameters, $\theta_{D,ki}$, we can identify explanatory functions that are significant in describing the bias in the deterministic model.

2.2   Description of Platform System

The platforms of interest are supported by four piles and installed in water depths between 20 meters and 300 meters. We predict deformation (drift) demands on the support structure and drill pipe subject to wave and current loading, as these usually represent the dominant environmental conditions (Xiaoyu and Hongnan, 2010). Although the supporting piles and jacket support structure are often symmetric, the equipment and structural components on the platform deck are usually asymmetric. In

addition, accidental eccentricity of the center of mass and center of rigidity is typically unavoidable due to many uncertain factors. This platform asymmetry is captured by a shift in the platform's center of mass (CM) and/or center of rigidity (CR) away from the geometric center (GC), as shown in Figure 2-1. For this system, X_m and X_R are the coordinates of the CM and CR along the x-axis, and Y_m and Y_R are the coordinates of the CM and CR along the y-axis. This formulation allows for eccentricity of different magnitudes and different directions. The eccentricity between the CR and CM will cause a coupled torsional-translational response, even though the forces acting on the structure only act in the translational direction. The rotation of the platform is assumed to occur about the CR as discussed by Tabatabaei (2011).
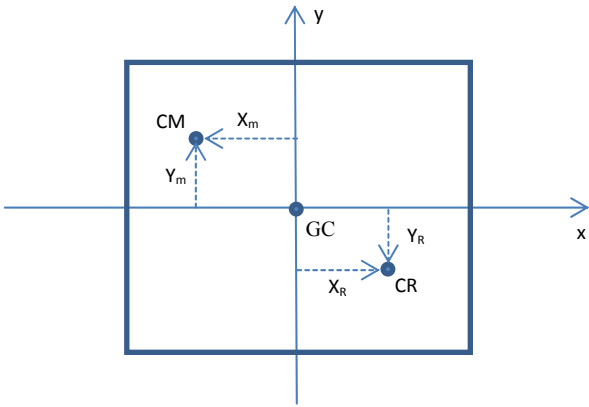

Figure 2-1. Plan view of asymmetric platform deck.

The offshore platforms studied in this paper are assumed to have a symmetric plan; that is, the length of the deck is the same in both the x-direction and y-direction.

11

Furthermore, the lateral stiffness of the platform is assumed to be equivalent in the x-direction and y-direction. Table 2-1 lists all structural, material, and loading parameters used to define a given platform configuration and their descriptions.

Table 2-1. Key design parameters.

Design Variable	Description	Units
d	Water depth	m
H	Wave height	m
T	Wave period	sec
v	Current velocity	m/sec
m	Platform mass	kg
L	Platform deck length	m
X_r	CR x-coordinate	m
Y_r	CR y-coordinate	m
X_m	CM x-coordinate	m
Y_m	CM y-coordinate	m
k_x	Lateral stiffness of platform	N/m
k_θ	Torsional stiffness of platform	N-m/rad
D	Diameter of platform legs (piles)	m
h	Height from seabed to platform deck	m
c	Clearance (height from sea level to platform deck)	m
R	Distance to CR from drill pipe or platform leg	m
r	Distance between CR and CM	m
CR	Distance between CR and GC	m

Figure 2-2 shows the asymmetric platform model under the combined wave and current environmental loadings (Xiaoyu and Hongnan 2010). Following Xiaoyu and Hongnan (2010), this offshore platform is simplified as a single-story model with two

translational and one torsional degrees of freedom (DOFs), and it is assumed to respond in the elastic range only. These simplifications and assumptions are made for two reasons: (1) This model is fairly simple and straightforward to analyze. The relative ease of analysis and interpretation of a single-story model allows for better understanding of the results. Thus, different parameters and characteristics of the asymmetric platform can be easily investigated. (2) The first three modes of the platform (two lateral orthogonal modes and one rotational mode) control a large portion of the response of the platform. In addition, the wave and current action is assumed to coincide with the positive x-axis. This assumption is made due to the fact that orientation of the platform with respect to the wave and current forces does not affect the model results; only the positions of the CM and CR That is, altering the positions of the CM and CR in the model (developed in Section 2.5.2) can effectively "rotate" the platform with respect to the wave and current incidence. Because the virtual experiment database will consider a wide range of CM and CR positions, the results of this study essentially capture all wave and current incidence angles.
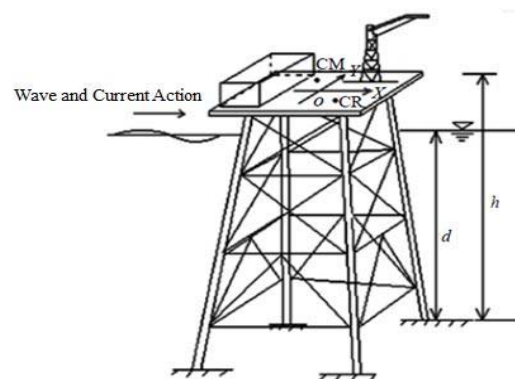

Figure 2-2. Simplified platform model and environmental actions.

13

It is also important to note that the model described above is very idealized. We have made several simplifications and do not account for structural nonlinearities. In turn, the results of this study would most likely be applicable during the preliminary or conceptual stages of a project and give an approximation of the structure's reliability based on key design parameters.

2.3   Deterministic Demand Model

An ideal deterministic model $\hat{d}_k(x, w)$ should be simple, accurate, and commonly accepted in practice. Therefore, we will use an equivalent static analysis of the offshore jacket platforms as the deformation deterministic model, as outlined by Chopra (2006). This model defines a vector of statically applied external forces on the stiffness component of the offshore platform. The equivalent static analysis can be formulated as

$$\begin{Bmatrix} f_{Sx} \\ f_{Sy} \\ f_{S\theta} \end{Bmatrix} = [K] \begin{Bmatrix} u_x \\ u_y \\ u_\theta \end{Bmatrix} \tag{2.3}$$

where f_{Sx}, f_{Sy}, and $f_{S\theta}$ are the statically applied external forces and moments in the x-direction, y-direction, and in the θ-direction (about the axis of rotation), respectively, K is the stiffness matrix of the asymmetric system, and u_x, u_y, and u_θ are the translator displacements of the geometric center (GC) along the x and y axes, and the rotation of the GC in the horizontal plan, respectively. Since we assume the wave and current incidence to coincide with the positive direction of the x axis, we can conclude that $f_{Sy} = 0$ and $f_{S\theta} = 0$. For the purposes of this model, f_{Sx} is defined as the maximum hydrodynamic force due to wave and current action that occurs over a specified time,

14

given a set of loading conditions. Wave and current forces are estimated using the Morison equation and drag equation, respectively, in same manner as illustrated below in Section 2.5.2. The stiffness matrix of the asymmetric platform is formulated following Xiaoyu and Hongnan (2010) as

$$\boldsymbol{K} = \begin{bmatrix} K_x & 0 & -K_x Y_R \\ 0 & K_y & K_y X_R \\ -K_x Y_R & K_y X_R & \left(K_\theta - K_x Y_m^2 - K_y X_m^2 + 2K_x Y_m Y_R + 2y K_y X_m X_R\right) \end{bmatrix} \quad (2.4)$$

where, K_x, K_y, and K_θ are the system stiffness in the x direction, y-direction, and rotational stiffness, respectively, X_m and Y_m are the coordinates of the center of mass (CM), and X_R and Y_R are the coordinates of the center of rigidity (CR) as shown in Figure 2-1.

This equivalent static model assumes the structure primarily responds in its fundamental mode, and does not account for significant torsional behavior well (Chopra 2006).

2.4   Model Correction

As defined earlier, the correction term $\gamma_D(\boldsymbol{x}, \boldsymbol{w}, \boldsymbol{\theta}_D)$, is intended to correct the bias in the deterministic model, $\hat{d}(\boldsymbol{x}, \boldsymbol{w})$. The linear form illustrated in Eq. (2.2) will be used for the correction term. The explanatory functions, $h_i(\boldsymbol{x}, \boldsymbol{w})$, should be selected to improve the accuracy of the prediction with respect to $\hat{d}(\boldsymbol{x}, \boldsymbol{w})$. Therefore, the terms that are thought to be missing or misrepresented from $\hat{d}(\boldsymbol{x}, \boldsymbol{w})$ can be selected as explanatory functions (Gardoni et al. 2002). Also, rules of mechanics and structural dynamics can guide in formulating the explanatory functions. It is also important to note that $h_i(\boldsymbol{x}, \boldsymbol{w})$ should

15

be dimensionless, so that $\theta_{D,i}$ are dimensionless. We select the following explanatory functions: $h_1(x, w) = 1$ to correct possible constant bias in the deterministic model that is independent of x and w, and $h_2(x, w) = \hat{d}(x, w)$ to capture any over-estimation or under-estimation in the deterministic model. To capture other factors influencing the bias in the deterministic model, additional explanatory functions are considered that include material properties, structural dimensions, and environmental loading variables.

A Bayesian inference using experimental data is used to approximate the unknown model parameters, $\theta_{D,i}$. Due to lack of existing experimental data needed for the statistical analysis, virtual data are generated by conducting detailed dynamic analyses of asymmetric offshore jacket platforms. We generate a database from the results of these experiments to conduct the statistical analysis required to estimate the model parameters.

2.5 Virtual Experiment Data

This study uses computer-based simulations to calculate the response of offshore jacket platforms. The term "virtual experiment" herein refers to a dynamic analysis of a specific platform configuration. A set of representative offshore platform configurations are used to compute virtual experiment data. This data is later used to calibrate the probabilistic demand model. The representative configurations are selected as to maximize their information content while minimizing the computational costs of the dynamic analyses by performing an experimental design. The experimental design is conducted by using a Latin hypercube sampling technique.

16

2.5.1 Latin Hypercube Sampling

The experimental design with virtual experiments differs from classical experimental design due to the deterministic nature of the computer-based simulations associated with virtual experiments. Therefore, there is no random error, and replication is unnecessary (Simpson et al. 2001). As stated by Simpson et al. (2001), the design space is defined as the region bounded by the upper and lower limits of each input variable, and the sample points should be chosen to fill the design space such that they spread as far from each other as possible. Many "space filling" methods exist. This study employs the Latin hypercube sampling technique introduced by McKay et al. (1979) to determine the representative configurations of the offshore platform. Latin hypercube sampling maximizes the minimum distance between the design points and evenly spaces each design point in its range to give a good coverage of the design space. This ensures the experimental design database contains results from evenly spaced representative configurations of offshore platforms within the design space. The input variables used to characterize each platform and their ranges are shown in Table 2-2. The practical rule of approximately 5 samplings per design variable is used. Therefore, 63 platform configurations are generated. Within each of these configurations, eight different values of R, the distance from the axis of rotation to the point where the platform response is calculated, are considered. This results in a total of 504 configurations that are considered. It is important to note that these configurations are not intended to correspond to any existing offshore platforms.

Table 2-2. Ranges of design parameters for typical offshore platforms.

Design Parameter	Range
Wave height, H	1-20 m
Wave period-to-wave height ratio, $T/\sqrt{H}$	3.6-5.0 sec/m$^{1/2}$
Water depth, d	20-300m
Platform mass, m	2x10^6-15x10^6 kg
Deck length (x and y direction), L	20-100 m
CR x-coordinate-to-deck length ratio, X_r/L	-0.25-0.25 %
CR y-coordinate-to-deck length ratio, Y_r/L	-0.25-0.25 %
CM x-coordinate-to-deck length ratio, X_m/L	-0.25-0.25 %
CM y-coordinate-to-deck length ratio, Y_m/L	-0.25-0.25 %
Natural frequency of platform (squared), k_x/m	1-30 (rad/sec)^2
Natural rotational frequency of platform (squared), $k_\theta/(m \cdot r^2)$	1-30 (rad/sec)^2
Clearance, c	5-20 m
Current velocity, v	0.03-2.5 m/sec
Platform leg diameter, D	0.5-2.0 m

2.5.2   *Analytical Modeling*

The dynamic analytical models are formulated to allow for the torsional behavior of the offshore platforms. A differential equation of motion is used to perform a linear dynamic analysis and model the dynamic responses as described by Xiaoyu and Hongnan (2010). This equation can be written in matrix form as follows:

$$[\boldsymbol{M}]\begin{Bmatrix}\ddot{x}\\\ddot{y}\\\ddot{\theta}\end{Bmatrix} + [\boldsymbol{C}]\begin{Bmatrix}\dot{x}\\\dot{y}\\\dot{\theta}\end{Bmatrix} + [\boldsymbol{K}]\begin{Bmatrix}x\\y\\\theta\end{Bmatrix} = \begin{Bmatrix}F_x\\F_y\\F_\theta\end{Bmatrix} \qquad (2.5)$$

where $[\boldsymbol{M}]$, $[\boldsymbol{C}]$, and $[\boldsymbol{K}]$ are the mass, equivalent damping, and stiffness matrices, x, $\dot{x}$, and $\ddot{x}$ are the displacement, velocity, and acceleration of the structure in the x-direction,

y, $\dot{y}$, and $\ddot{y}$ are the displacement, velocity, and acceleration of the structure in the y-direction, θ, $\dot{\theta}$, and $\ddot{\theta}$ are the angular rotation, angular velocity, and angular acceleration of the structure about the z-axis, and F_x, F_y, and F_θ are the forcing functions in the x-direction, y-direction, and about the z-axis, respectively. The origin of the coordinate system is located at the geometric center (GC) of the deck of the offshore platform. The third degree of freedom in this differential equation of motion, the rotation about the z-axis, is included to examine the torsional effects of the mass and rigidity eccentricity of the platform. This is achieved through the formulation of the mass and stiffness matrices, as shown below:

$$M = \begin{bmatrix} m & 0 & -mY_m \\ 0 & m & mX_m \\ -mY_m & mX_m & m(r^2 + X_m^2 + Y_m^2) \end{bmatrix} \tag{2.6}$$

$$K = \begin{bmatrix} K_x & 0 & -K_xY_R \\ 0 & K_y & K_yX_R \\ -K_xY_R & K_yX_R & (K_\theta - K_xY_m^2 - K_yX_m^2 + 2K_xY_mY_R + 2yK_yX_mX_R) \end{bmatrix} \tag{2.7}$$

where m is the equivalent mass of the platform deck, r is the radius of gyration of the mass about a vertical axis passing through the center of mass (CM), K_x, K_y, and K_θ are the system stiffness in the x direction, y-direction, and rotational stiffness, respectively, X_m and Y_m are the coordinates of the CM, and X_R and Y_R are the coordinates of the center of rigidity (CR), as shown in Figure 2-1. The equivalent damping matrix will be computed using Raleigh damping, as shown below:

$$[C] = \alpha[M] + \beta[K] \tag{2.8}$$

where α and β are the Raleigh damping coefficients.

The forcing functions in Eq. (2.5) are a result of the hydrodynamic (wave and current) loading on the offshore platform's support structure. For the purposes of this study the wave and current forces are assumed to be unidirectional and act in the positive x-direction only. The hydrodynamic wave forces on the offshore platforms are estimated by the Morison equation, which accounts for the relative motion of the structure and water particles (Morison et al. 1950). The Morison equation gives the wave force on the legs of the platform per unit length as:

$$f_w = C_D \frac{\rho D}{2} |u - \dot{x}|(u - \dot{x}) + C_m \rho \frac{\pi D^2}{4} (\dot{u} - \ddot{x}) + \rho \frac{\pi D^2}{4} \dot{u} \qquad (2.9)$$

where C_D and C_m are the drag coefficient and added mass coefficient of the platform leg, respectively, ρ is the density of the seawater, D is the diameter of the platform leg, u and $\dot{u}$ are the undisturbed acceleration and velocity of the sea water, and $\dot{x}$ and $\ddot{x}$ are the acceleration and velocity of the platform leg at a certain elevation. We assume the drag and added mass coefficients to be 1.2 and 1.0, respectively. Integrating this equation over the water depth yields the total force acting on one platform leg. It is important to note that certain terms resulting in the simplification of Eq. (2.9) are functions of the structure's acceleration and velocity. These terms are known as the added mass term and wave damping term, respectively, and they are included in the mass and damping matrices from Eq. (2.5), as shown below

$$M = \begin{bmatrix} m + n \int_{-d}^{0} C_m \rho \frac{\pi D^2}{4} dz & 0 & -mY_m \\ 0 & m + n \int_{-d}^{0} C_m \rho \frac{\pi D^2}{4} dz & mX_m \\ -mY_m & mX_m & m(r^2 + X_m^2 + Y_m^2) \end{bmatrix} \quad (2.10)$$

$$C = \begin{bmatrix} C_{11} + n \int_{-d}^{0} C_D \frac{\rho D}{2} \bar{a} \, dz & 0 & C_{13} \\ 0 & C_{22} + n \int_{-d}^{0} C_D \frac{\rho D}{2} \bar{a} \, dz & C_{23} \\ C_{31} & C_{32} & C_{33} \end{bmatrix} \quad (2.11)$$

where n is the number of platform legs.

The wave kinematics are estimated by linear wave theory. This model is based on the solution of the Laplace equation in terms of the velocity potential given by the following equation (Dean and Dalrymple 1991):

$$\varphi = a \frac{g}{\omega} \frac{\cosh(k(z + h))}{\cosh(kh)} \cos(kx - \omega t) \quad (2.12)$$

where φ is the velocity potential, a is the amplitude of the wave, ω is the frequency of the wave which is determined by solving the dispersion equation $\omega^2 = gk \tanh(kh)$, g is the gravitational acceleration, h is the water depth, and k is the wave number defined by $k = 2\pi/L$, where L is the wave length as shown in Figure 2-3. The horizontal water velocity, u, and acceleration, $\dot{u}$, is then calculated as $u = -\partial \varphi / \partial x$ and $\dot{u} = \partial u / \partial t$, respectively.
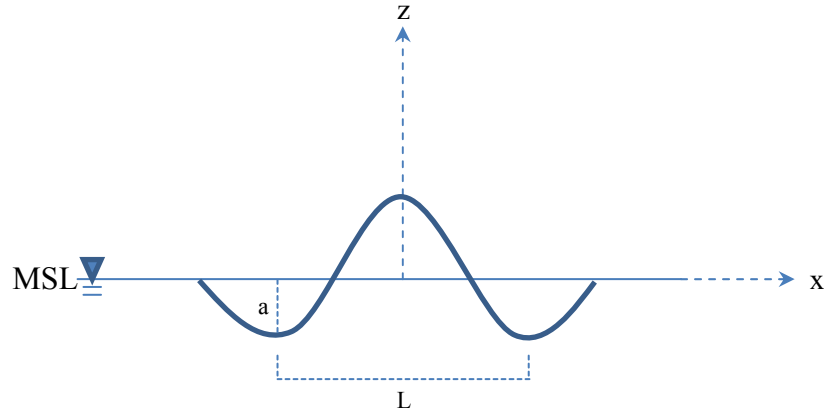
Figure 2-3. Schematic illustration of wave relative to mean sea level (MSL).

The hydrodynamic current forces on the platforms legs are estimated by the drag equation (Batchelor 1967). We assume the current velocity to be constant with varying water depth. The drag equation gives the force on one leg of the platform as:

$$F_D = \frac{1}{2}\rho v^2 C_D A \tag{2.13}$$

where ρ is the density of the seawater, v is the horizontal current velocity, C_D is the drag coefficient as mentioned above, and A is the area of the orthographic projection of the platform leg perpendicular to the direction of the current.

The combination of wave and current forces results in the following forcing functions after accounting for the added mass and wave damping terms:

$$F_x = n \int_{-d}^{0} C_D \frac{\rho D}{2} \bar{a} \cdot u \, dz + n \int_{-d}^{0} C_M \rho \frac{\pi D^2}{4} \dot{u} \, dz + \frac{1}{2}\rho v^2 C_D A \tag{2.14}$$

where C_M is the inertia coefficient defined as $C_M = C_m + 1$.

Once the time history response for the 3 degrees of freedom in Eq (2.5) is known, the displacement at any point on the platform deck at any given time can be computed. We then assess the maximum drift that occurs at every point on the platform deck over the response time. These values can be displayed in contour form as shown in the example contour below in Figure 2-4. The axis of rotation can typically be identified as within the area of the smallest maximum drift values. It can be seen that as the point at which the drift is computed moves further away from the axis of rotation (located at the CR), the maximum drift at that point increases. This is a result of the torsional response of the platform. This information is used to allow for the computation of the drift of the drill pipe when located at various points on the platform deck (as opposed to just at the axis of rotation) as well as the drift at the legs of the platform. It is important to note that similar contours and drift calculations are computed from the responses of the three degrees of freedom in the deterministic model, which is formulated in Section 2.3.
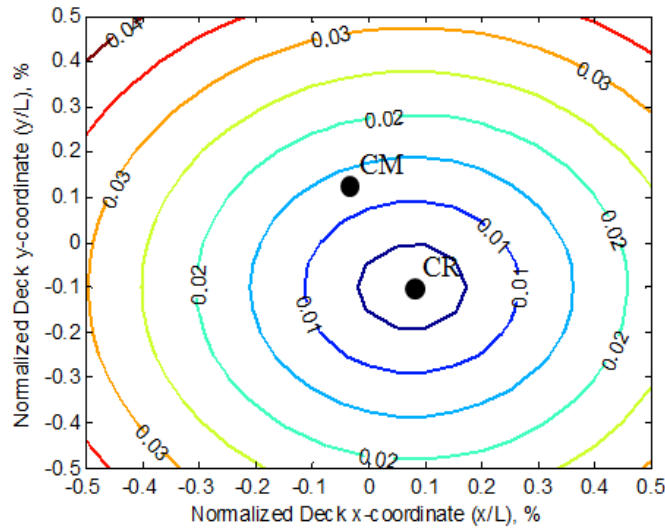
Figure 2-4. Example maximum drift contour of platform deck.

2.5.3 Equality and Lower Bound Data

The data from each virtual experiment can be classified as either equality data or lower bound data, as shown by Gardoni et al. (2002) and Ramamoorthy et al. (2006). An equality datum is such that the quantity of interest (i.e. deformation) as calculated by the virtual experiments is believed to be accurate. When an accurate virtual experiment value is unavailable and only a value that is a lower bound to the true value is available, a lower bound datum exists. In the context of this study, when the deformations in the dynamic analyses are relatively large, the results are deemed no longer reliable. This is due to the structural nonlinearities associated with large displacements that are not accounted for in the linear dynamic model. Therefore, we consider a 5% lower bound on the drift of the platform, such that if the maximum drift during one time history analysis

is less than 5%, the deformation data is classified as equality data. If the maximum drift during one time history analysis exceeds this 5% threshold, then we consider a 5% drift as the lower bound datum, and the data is classified as lower bound data. Two types of lower bound data result from the experimental simulations, as discussed by Bai et al. (2011): lower bound I data and lower bound II data. For lower bound cases, the first time at which any point on the offshore platform deck exceeds the 5% drift threshold is determined based on the time history response of the platform. The threshold drift is then taken as the lower bound I data for that point on the platform deck. Similarly, the maximum drift at all other points on the platform deck up to that time are considered as lower bound II data. The lower bound II data points will be less than the 5% drift threshold, but still considered lower bound. In Figure 2-5, the blue dots represent equality data, while the green triangles and red squares represent lower bound Type I and Type II data, respectively. The left chart of Figure 2-5 displays the data from the point on each platform configuration that had the largest drift over the time history response, while the right chart displays data from all other points on each platform configuration. The triangles indicate the data points that first exceeded 5% drift (Type I), and the squares indicate the corresponding lower bound data for other points (Type II). It is important to note that Figure 2-5 displays the uncensored data. With this lower bound datum approach, the data from the experiments that result in large deformations are incorporated without allowing inaccurate results to influence the model parameters.
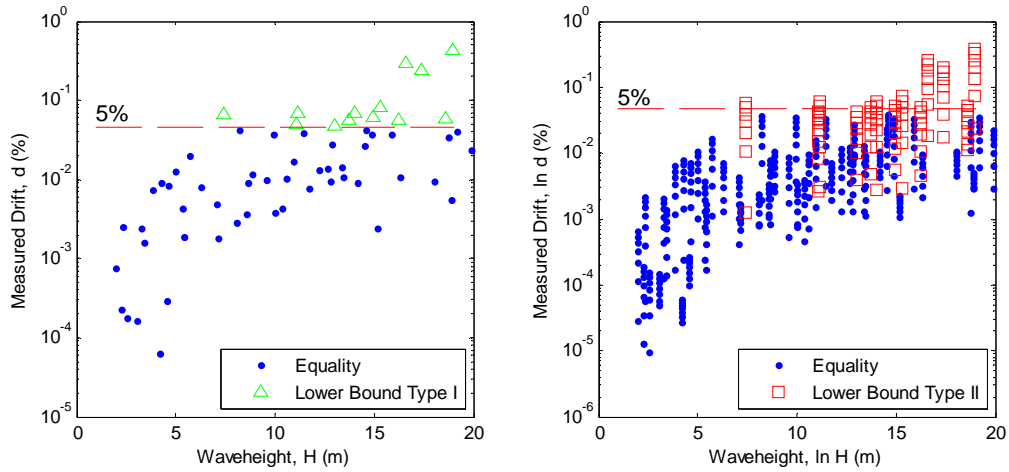
Figure 2-5. Lower bound Type I and Type II drift values.

2.6   Probabilistic Demand Model

The unknown model parameters of the probabilistic demand model for deformation demands on offshore platforms due to environmental loadings are estimated by generating a virtual experiment database, as discussed in Section 2.5. The unknown model parameter selection process should create a demand model that is unbiased, accurate, and easily implementable (Gardoni et. al 2002). In addition, the model selection process should aim to develop a parsimonious demand model (i.e., have as few explanatory functions, h_i, as possible) to avoid loss of precision of the estimated parameters and the model due to inclusion of unimportant predictors.

2.6.1   Bayesian Parameter Estimation

The model parameters, $\mathbf{\Theta}_{D,k}$, are estimated using a Bayesian approach based on the following updating rule (Box and Tiao 1992):

$$f(\mathbf{\Theta}_{D,k}) = \kappa L(\mathbf{\Theta}_{D,k}) p(\mathbf{\Theta}_{D,k}) \tag{2.15}$$

where $f(\mathbf{\Theta}_{D,k})$ = posterior distribution that represents the updated distribution of $\mathbf{\Theta}_{D,k}$,

$p(\mathbf{\Theta}_{D,k})$ = prior distribution of $\mathbf{\Theta}_{D,k}$ representing our state of knowledge about $\mathbf{\Theta}_{D,k}$

prior to conducting the virtual experiments, κ = normalizing factor, and $L(\mathbf{\Theta}_{D,k})$ =

likelihood function representing the objective information about $\mathbf{\Theta}_{D,k}$ that comes from

the set of virtual experiments. The likelihood function is a function that is proportional to

the conditional probability of observing the virtual experiment results for given values of

model parameters, $\mathbf{\Theta}_{D,k}$. Following Gardoni et al. (2002), the likelihood function,

incorporating lower bound data, is written as

$$L(\mathbf{\theta}_k, \sigma_k) \propto \prod_{failure\ data} \left\{ \frac{1}{\sigma_k} \varphi \left[\frac{r_{ik}(\mathbf{\theta}_k)}{\sigma_k} \right] \right\} \times \prod_{lower\ bound\ data} \Phi \left[-\frac{r_{ik}(\mathbf{\theta}_k)}{\sigma_k} \right] \tag{2.16}$$

where $\varphi(\cdot)$ and $\Phi(\cdot)$ denote the standard normal probability density function and

cumulative distribution functions, respectively, and r_{ik} is defined as $r_{ik}(\mathbf{\theta}_k) = D_{ik} -$

$\hat{d}_k(\mathbf{x_i}, \mathbf{w_i}) - \gamma_k(\mathbf{x_i}, \mathbf{w_i}, \mathbf{\theta}_k)$, D_{ik} = observed value for k^{th} demand for a given $\mathbf{x_i}$ and $\mathbf{w_i}$.

The prior distribution of $\mathbf{\Theta}_{D,k}$, $p(\mathbf{\Theta}_{D,k})$, may incorporate any information about $\mathbf{\Theta}_{D,k}$

that is based on our engineering judgment or past experience. When there is no prior

information about $\mathbf{\Theta}_{D,k}$, a noninformative prior distribution should be used so that

inferences are affected by virtual experiment data results only. Once the posterior

distribution of $\mathbf{\Theta}_{D,k}$ is known, the mean vector and covariance matrix, denoted $\mathbf{M_\Theta}$ and

$\mathbf{\Sigma_{\Theta\Theta}}$, respectively, can be calculated.

2.6.2   Model Parameter Estimation

The accuracy of the probabilistic demand model in Eq. (2.1) can be represented by the model's standard deviation, σ. Therefore, the posterior mean of σ can be used to identify the most accurate model from among a set of parsimonious model candidates. We begin the model selection process with a comprehensive candidate form of $\gamma_D(x, w, \theta_D)$ containing all considered explanatory functions presented in Table 2-3 and then simplify it by removing unimportant terms. This is known as a step-wise deletion process, as described by Gardoni et al. (2002). The first step of the step-wise deletion process is to compute the posterior statistics of the unknown model parameters $\theta = (\theta_1, \dots, \theta_p)$ and σ_D using the Bayesian approach described above. Next, we identify the term $h_i(x, w)$ whose coefficient, θ_i, has the largest posterior coefficient of variation. This term is the least informative of all candidate explanatory functions, so it may be dropped from the demand model. Finally, the reduced model is assessed by estimating its unknown parameters using the Bayesian approach. The reduced model is accepted if the posterior mean of σ_D has not increased by an unacceptable amount, and the deletion process may be repeated. Otherwise, the reduction was not desirable, and the model form before the reduction is as parsimonious as possible. This process achieves a compromise between model simplicity and model accuracy.

Table 2-3. Comprehensive list of explanatory functions.

Explanatory Function	Formula
h_1	1
h_2	$ln[d]$
h_3	$ln[H/h]$
h_4	$ln[k_x \cdot h \cdot D/H]$
h_5	$ln[k_\theta/(mg \cdot R)]$
h_6	$ln[k_x \cdot R/mg]$
h_7	$ln[k_\theta/(mg \cdot CR)]$
h_8	$ln[R/L]$
h_9	$ln[r/h]$
h_{10}	$ln[\omega/\omega_n]$
h_{11}	$ln[\omega/\omega_{\theta n}]$
h_{12}	$ln[\omega \cdot R/(\omega_n \cdot L)]$
h_{13}	$ln[\omega \cdot R/(\omega_{\theta n} \cdot L)]$

We select the following explanatory functions: $h_1(x, w) = 1$ to capture potential constant bias in the deterministic model that is independent of x and w, and $h_2(x, w) = \hat{d}(x, w)$ to capture any over-estimation or under-estimation in the deterministic model. Additional explanatory functions are also considered to capture possible dependence of residuals on parameters which are not included in the deterministic model. A complete list of all considered explanatory functions is displayed in Table 2-3. The structural, loading, and material properties used to define the explanatory functions are listed in Table 2-1. We select $h_3(x, w) = \ln[H/h]$ to account for possible dependencies of the residuals on the wave height, as it is typically the loading parameter with the greatest effect on deformation. To capture the possible effect of the platform's lateral stiffness,

29

we select $h_4(x, w) = \ln[(k_x hD)/H]$ and $h_6(x, w) = \ln[(k_x R)/mg]$. To account for influences of the torsional stiffness, we choose $h_5(x, w) = \ln[k_\theta/(mg \cdot R)]$ and $h_7(x, w) = \ln[k_\theta/(mg \cdot CR)]$. Furthermore, h_5, h_6, and h_7 also account for effects due to the mass of the platform. We select $h_8(x, w) = \ln[R/L]$ to account for dependencies on the radial distance from the CR at which the drift is calculated at. To explore the effect of the distance between the CR and CM, we choose $h_9(x, w) = \ln[r/h]$. To capture the possible effects of the wave frequency in relation to the natural frequency of the structure, we select $h_{10}(x, w) = \ln[\omega/\omega_n]$ and $h_{12}(x, w) = \ln[\omega R/(\omega_n L)]$. Finally, we select $h_{11}(x, w) = \ln[\omega/\omega_{\theta n}]$ and $h_{13}(x, w) = \ln[\omega R/(\omega_{\theta n} L)]$ to account for influences of the wave frequency in relation to the torsional natural frequency of the structure. It is important to note that these explanatory functions are dimensionless, and therefore the parameters $\boldsymbol{\theta}$ are also dimensionless. Additional explanatory functions could also be selected, but we believe that the thirteen selected ones will capture all significant factors that influence the drift demand of the offshore platform.

Since no prior information on the unknown parameters $\boldsymbol{\Theta}_\delta = (\boldsymbol{\theta}_\delta, \sigma_\delta)$ is available before the virtual experiments are conducted, a non-informative prior distribution of the form $p(\boldsymbol{\theta}_\delta, \sigma_\delta) \propto \sigma_\delta^{-1}$ is used (Box and Tiao 1992). Figure 2-6 summarizes the step-wise term deletion for the deformation demand model. The posterior coefficients of variation of the model parameters θ_i at each step are shown as solid dots, and the posterior means of the model standard deviation σ at each step are shown as open squares.
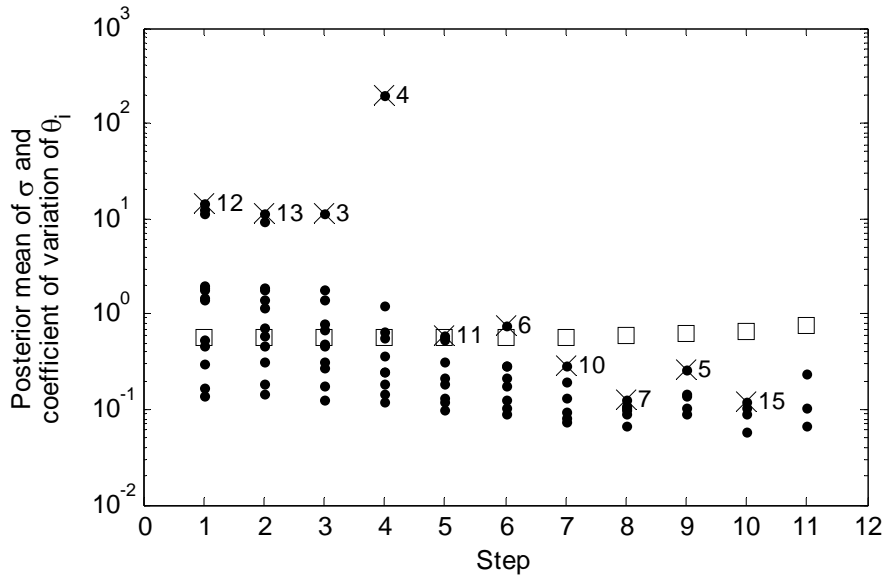
30

Figure 2-6. Step-wise deletion process for deformation demand model.

At the first step, with the model containing all candidate explanatory functions, the posterior mean of σ is 0.5718 and the parameter with the largest COV is θ_{12} with a COV of 14.39. Therefore, the model is reduced by dropping the term $\theta_{12}h_{12}(\boldsymbol{x},\boldsymbol{w})$. In Figure 2-6, the cross symbol indicates that this term was dropped. Now, we proceed to step 2 and assess the new 13-parameter model. The posterior mean of σ remains unchanged at 0.5718. Because σ has not increased by an unacceptable amount, the model has not significantly deteriorated, and now the parameter with the highest COV is θ_{13}. The model is reduced by dropping the term $\theta_{13}h_{13}(\boldsymbol{x},\boldsymbol{w})$ and we continue the same procedure. After 10 steps, we have a model with a posterior mean of σ of 0.6365. The parameter with the highest COV is θ_9, and we drop the term $\theta_9h_9(\boldsymbol{x},\boldsymbol{w})$. At step 11, the new posterior mean of σ is 0.7542. This increase in the standard deviation of the model

31

is deemed unacceptable and is an indication that removing the term $\theta_9 h_9(x, w)$ deteriorated the quality of the model. Therefore, the model form before the reduction of $\theta_9 h_9(x, w)$ is as parsimonious as possible. Stopping at that point, we are left with the terms $\theta_1 h_1(x, w)$, $\theta_2 h_2(x, w)$, $\theta_8 h_8(x, w)$, and $\theta_9 h_9(x, w)$, and the posterior mean of σ is 0.657.

2.6.3   Deformation Demand Model

The probabilistic deformation demand model is formulated in terms of the natural logarithm of the drift demand. The drift demand is defined as the deformation demand at the deck of the offshore platform, Δ, normalized by the height of the platform, h. A logarithmic transformation is used to satisfy the homoscedasticity and normality assumptions (i.e. $D_\delta = ln(\Delta/h)$ and $\hat{d}_\delta = ln(\hat{\Delta}/h)$). After performing the step-wise deletion model selection process, we are left with the final probabilistic deformation demand model, written as:

$$D_\delta(x, w, \theta_\delta) = \hat{d}(x, w) + \theta_1 + \theta_2 \hat{d}(x, w) + \theta_8 \ln\left(\frac{R}{L}\right) + \theta_9 \ln\left(\frac{r}{h}\right) + \sigma\varepsilon \quad (2.17)$$

2.6.4   Model Assessment

Table 2-4 gives the posterior statistics of $\mathbf{\Theta}_\delta = (\theta_1, \theta_2, \theta_8, \theta_{9,}\sigma)$ of the reduced probabilistic model. Some important observations can be made from these statistics: (1) The positive mean of θ_1 suggests that, independent of structural and loading parameters x and w, the selected deterministic model, $\hat{d}(x, w)$, tends to underestimate the

32

deformation demand on the offshore platform. (2) The positive posterior estimate of θ_8 indicates that the deterministic model tends to underestimate the torsional response of the platform (the "twisting" of the platform contributes more to the deformation demand as the value of R increases). This is expected, due to the fact that the deterministic model does not account for higher modes of response well, as illustrated in Section 2.3. Similarly, the positive estimate of θ_9 indicates that the deterministic model does not properly account for the eccentricity between the CR and CM that induces the torsional vibration. Once again, this is expected due to the shortcomings in the deterministic model of the higher mode response estimations.

Table 2-4. Posterior statistics of parameters in demand model.

Parameter	Mean	Standard deviation	θ_1	θ_2	θ_8	θ_9	σ
				Correlation Coefficient			
θ_1	1.842	0.193	1				
θ_2	-0.198	0.023	0.719	1			
θ_8	0.451	0.026	0.194	0.008	1		
θ_9	0.470	0.043	0.524	-0.162	-0.003	1	
σ	0.657	0.026	-0.024	-0.084	-0.052	0.063	1

A comparison between the measured (experimental data) and predicted values of drift demands for the asymmetric offshore platforms based on the deterministic model (left chart) and the probabilistic model (right chart) is displayed in Figure 2-7. On the right chart, median predictions ($\varepsilon = 0$) of the probabilistic model are displayed. The equality data are shown as solid dots, the Type II lower bound data are inscribed in open

squares, and the Type I lower bound data are inscribed in open triangles. The dashed line in both charts depicts the 1:1 line, and the dotted lines in the right chart delimit the region within one standard deviation of the median.
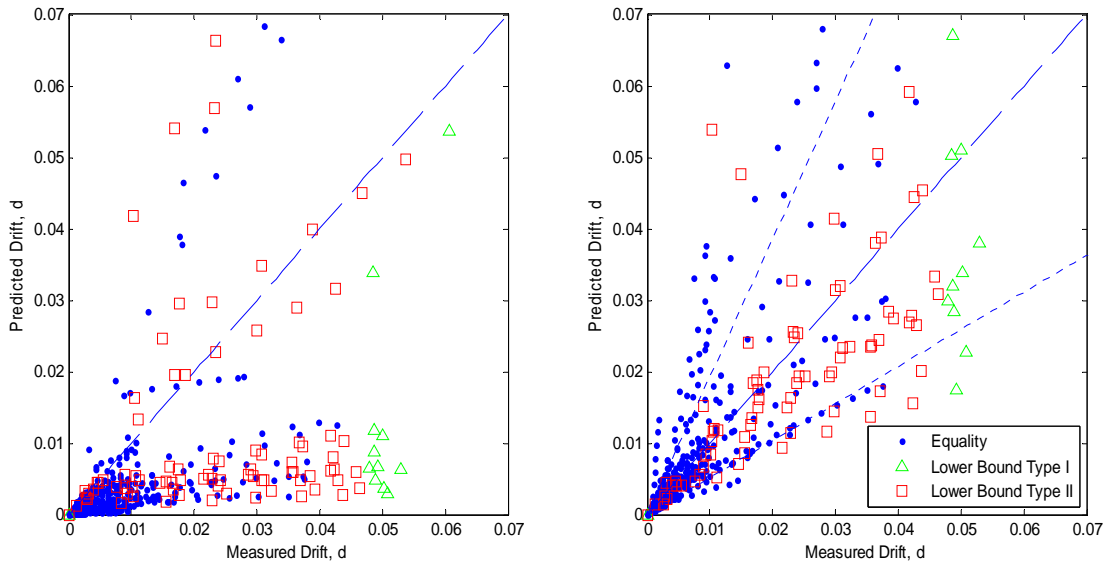

Figure 2-7. Comparison between measured and predicted demands based on deterministic (left) and probabilistic (right) models.

The deterministic model on the left is clearly biased to the non-conservative side (under-estimates the deformation of the platform) since most of the data lie below the 1:1 line. For a perfect model, the equality data should fall along the 1:1 line, and the lower bound data should lie above it. The chart on the right clearly shows that the probabilistic model corrects the bias that is apparent in the deterministic model. Most of the data fall within one standard deviation of the median prediction of the probabilistic

model. Some of the lower bound data points fall below the 1:1 line; this can be attributed to the fact that, for these platform configurations, the deterministic model predicts very small deformations while the experimental data show very large deformations. Therefore, because it contains the deterministic model, the probabilistic model still shows some of this trend, and several lower bound data points fall below the 1:1 line. It is clear that the probabilistic model corrects the bias inherent in the deterministic model and accounts for the prevailing uncertainties.

3. FRAGILITY ESTIMATES

3.1   Introduction

In this study, we define fragility as the conditional probability of failure for a given set of loading conditions, which we defined earlier as $\boldsymbol{w}$. Following Ditlevsen and Madsen (1996) and Gardoni et al. (2002), we let $g(\boldsymbol{x}, \boldsymbol{w}, \boldsymbol{\Theta})$ be a mathematical model that describes the deformation limit state for the platform. As defined earlier, $\boldsymbol{x}$ denotes a vector of measurable structural variables, $\boldsymbol{w}$ denotes a vector of external loading variables, and $\boldsymbol{\Theta}$ denotes a vector of model parameters. The deformation limit state functions for an offshore platform are formulated as

$$g(\boldsymbol{x}, \boldsymbol{w}, \boldsymbol{\Theta}) = C - D(\boldsymbol{x}, \boldsymbol{w}, \boldsymbol{\Theta}) \tag{3.1}$$

where C is a specified capacity for the deformation limit state, and $D(\boldsymbol{x}, \boldsymbol{w}, \boldsymbol{\Theta})$ is the probabilistic demand model developed previously. The limit state function is defined such that the event $\{g(\boldsymbol{x}, \boldsymbol{w}, \boldsymbol{\Theta}) \leq 0\}$ denotes attainment or exceedance of the deformation limit state. The fragility of the support structure can then be defined as

$$F(\boldsymbol{w}, \boldsymbol{\Theta}) = P[\{g(\boldsymbol{x}, \boldsymbol{w}, \boldsymbol{\Theta}) \leq 0\}|\boldsymbol{w}] \tag{3.2}$$

where $P[A|\boldsymbol{w}]$ is defined as the conditional probability of event A for the given values of variables $\boldsymbol{w}$. The randomness in $\boldsymbol{x}$, the inexact nature of $g(\boldsymbol{x}, \boldsymbol{w}, \boldsymbol{\Theta})$, and the uncertainty inherent in the model parameters $\boldsymbol{\Theta}$ cause uncertainty in the estimate of fragility

The predictive estimate of fragility, $\tilde{F}(\boldsymbol{w})$, is the expected value of $F(\boldsymbol{w}, \boldsymbol{\Theta})$ over the posterior distribution of $\boldsymbol{\Theta}$, and it incorporates the epistemic uncertainties inherent in

the model parameters by considering Θ as a random vector. Following Gardoni et al. (2002), a predictive estimate of the fragility can be formulated as

$$\tilde{F}(w) = P[\{g(x, w, \Theta) \le 0\}|w] \tag{3.3}$$

We calculate the predictive estimates of fragility through the use of Finite Element Reliability Using Matlab (FERUM). This software package uses Monte Carlo simulations to perform a fragility analysis on the deformation limit state function, where the unknown model parameters, $\boldsymbol{\theta} = (\theta_1, \theta_2, \theta_8, \theta_9)$, and error terms, σ and ε, in the demand model are considered as random variables. This method is used to construct fragility curves for specified capacities.

3.2   Fragility Estimates for an Example Asymmetric Offshore Platform

We now use the previously developed demand model to assess the fragility of an example asymmetric offshore platform. To conduct this, we consider a typical 4-leg offshore jacket platform installed in 160 m water depth. Important parameters for this example platform are provided in Table 3-1. A drift limit of 5% is considered as the deformation capacity for the drill pipe, which is located at a distance of 20 m ($R = 20$ m) from the CR. We define this configuration as the "baseline" configuration for future analyses. As discussed above, Monte Carlo simulations are used to develop the fragility curve for this capacity and configuration.

Table 3-1. Important parameters of the baseline platform configuration.

Parameter	Symbol	Value
Wave period	T	14 sec.
Current velocity	v	1.5 m/sec.
Water depth	d	160 m
Platform height	h	180 m
Platform deck length	L	65 m
Leg diameter	D	1.0 m
CR x-coordinate	X_r	5.25 m
CR y-coordinate	Y_r	8.00 m
CM x-coordinate	X_m	-3.00 m
CM y-coordinate	Y_m	7.50 m
Platform mass	m	8.38×10^6 kg
Lateral stiffness	k_x	1.25×10^8 N/m
Torsional stiffness	k_θ	5.6×10^{10} N·m/rad.

Figure 3-1 displays the predictive probability of failure (fragility) for the example offshore platform plotted as a function of wave height, H.
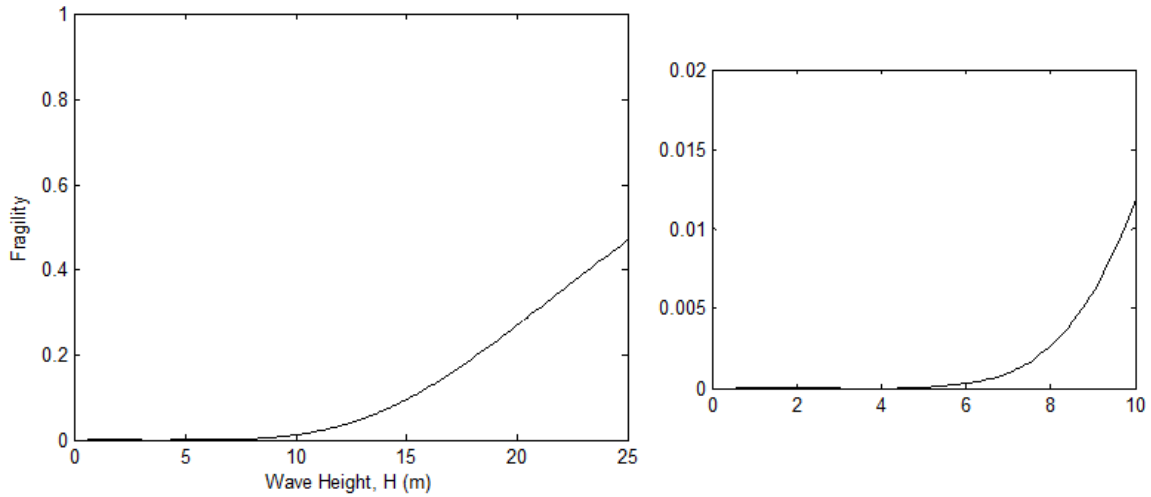
Figure 3-1. Predictive fragility estimate for
baseline configuration with 5% drift capacity.

3.2.1 Sensitivity Analysis

Next, we examine the sensitivity of altering important design parameters on the fragility

of the baseline offshore platform configuration. We consider three parameters that have

substantial effect on the limit state function: (1) r, the eccentricity existing between the

CM and CR, (2) R, the distance from the axis of rotation at which the drift is examined,

and (3) C, the given drift capacity for the structural member of interest.

Figure 3-2 displays the sensitivity of modifying the eccentricity between the CM

and CR on the baseline configuration. The black line denotes the baseline configuration

with an eccentricity of 17.5 m. This figure clearly shows that a greater degree of

asymmetry corresponds to a higher probability of failure. Moreover, ignoring the

asymmetry and assuming a symmetric platform is a very non-conservative assumption; the asymmetry of the structure must be considered when examining fragility.
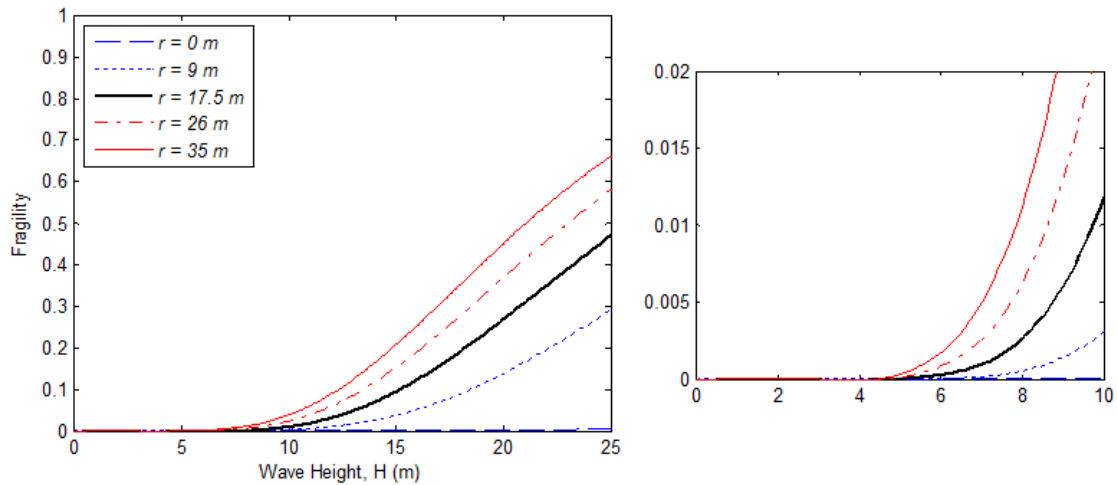

Figure 3-2. Sensitivity of altering platform eccentricity.

Next, the sensitivity of modifying R on the deformation reliability of the structural member at that location is investigated in Figure 3-3. The fragility estimate for $R = 20$ m, denoted by the black curve, corresponds to the baseline configuration. It can be seen that a greater distance to the axis of rotation corresponds to a higher probability of failure at that location due to excessive deformation. In other words, the closer the drill pipe is located to the center of rigidity, the smaller the probability of deformation failure.
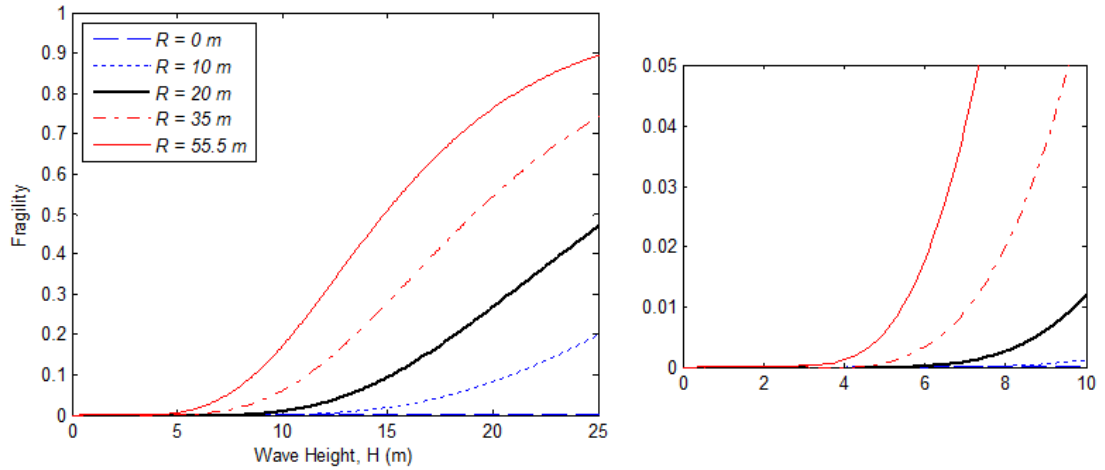
Figure 3-3. Sensitivity of altering drill pipe location.

Finally, the fragility of the baseline configuration platform is plotted against various drift capacity values, shown in Figure 3-4. It is important to note that because we specified a lower bound datum of 5% drift in the formulation of the probabilistic demand model, the fragility analyses for assumed capacities greater than 5% may not be accurate. As expected, a relative small capacity level corresponds to a much greater probability of failure.
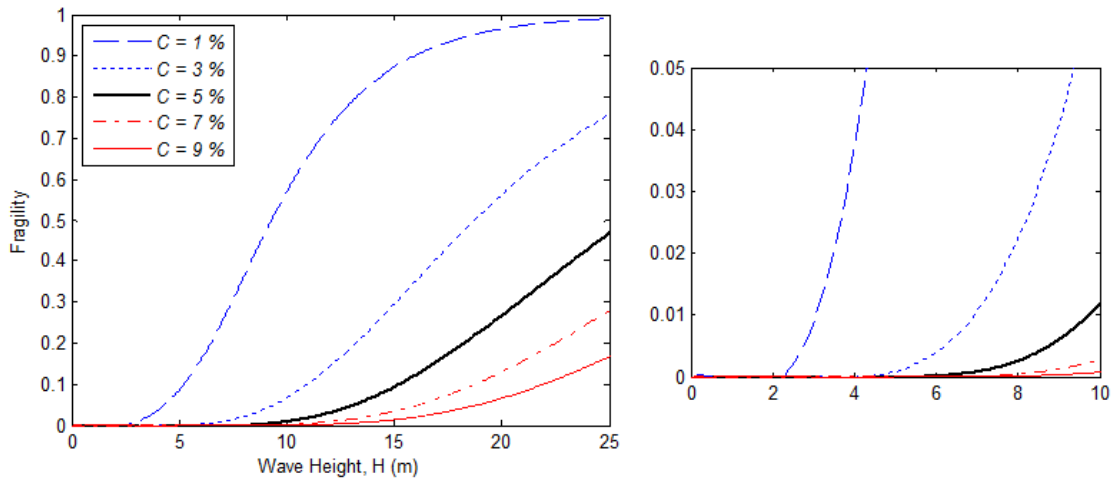
Figure 3-4. Sensitivity of altering drift capacity.

3.2.2 Ultimate Limit State Fragility Analysis

In Section 1.1, we defined the deformation of the platform legs as an ultimate limit state, as exceeding the structural deformation capacity of these members will result in ultimate failure of the platform. Now, we will use predictive fragility estimates to examine the probability of exceeding this ultimate limit state of the platform.

For this purpose, we will use the same baseline configuration as presented in Section 3.2. However, R is now magnitude of the distance from the CR to the platform leg that experiences the largest deformation. This is typically the leg that is farthest from the CR due to the torsional response of the asymmetric platform. In the case of the baseline configuration, this distance is 55.5 m. In addition, we will assume an ultimate drift capacity of 5%. The solid red line in Figure 3-3 displays the fragility curve for this configuration.

42

3.2.3   Serviceability Limit State Fragility Analysis

A serviceability limit state was also defined in Section 1.1 as the deformation of the drill pipe. Excessive drill pipe deformation will cause the offshore platform production operations to cease but will not cause ultimate structural failure; thus, we consider it as a serviceability limit state. We can also use fragility estimates to investigate this mode of failure.

Once again, we consider the baseline configuration. For serviceability, we assume a drift capacity of 5%. Figure 3-5 displays a predictive fragility contour of the platform deck, assuming the platform encounters a maximum wave height of 10 m. The x-axis corresponds to the x-coordinate position on the platform normalized with the length of the platform deck, and the y-axis corresponds to the y-coordinate position on the platform normalized with the length of the platform deck. The resulting contours lines are concentric circles around the CR, and the values on the contour lines denote the probability of failure. Figure 3-5 displays the contour for a given value of r (17.5 m). However, it is important to note that if we increase the asymmetry of the structure, we will still have concentric contours around the CR, but the fragility values will also increase. This fragility contour can be used to determine the optimal location or evaluate potential locations of the drill pipe in order to avoid a serviceability failure. It is clear that the optimal location for the drill pipe is at the CR. Moreover, the probability of failure can increase very quickly if there are even small errors in determining the drill pipe location.
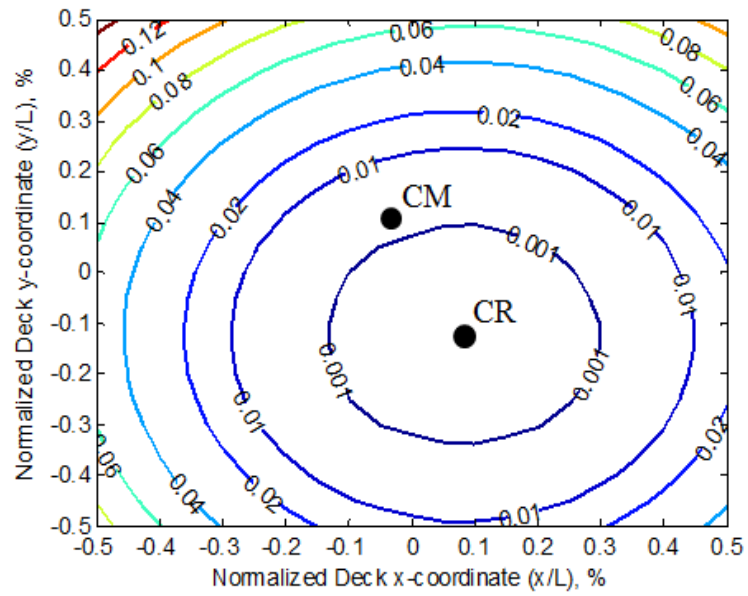
Figure 3-5. Fragility contour of platform deck.

4. CONCLUSIONS AND FUTURE WORK

4.1   Conclusions

The paper presents a Bayesian framework for developing probabilistic deformation demand models for asymmetric offshore jacket platforms subject to wave and current loads. The demand model properly accounts for uncertainties and is unbiased. In order to facilitate the use of the developed demand model in practice, the probabilistic model is formulated by adding correction terms to an existing deterministic deformation demand model. This properly corrects the inherent bias and enhances the accuracy of the deterministic model. The probabilistic model correction terms are constructed through a model selection process that considers a set of candidate explanatory functions which are chosen based on engineering judgment and an understanding of the underlying physical phenomena. The unknown parameters in the probabilistic model are estimated using a Bayesian updating method. The Bayesian approach was conducted using virtual experiment demand data obtained from time history analyses of representative platform configurations subject to wave and current forces. An experimental design procedure was used to develop 504 representative offshore platform configurations for analysis in the virtual experimentation. A comprehensive candidate form of the probabilistic model, which includes all considered explanatory functions, is considered, and a step-wise deletion process is used to filter out the least informative explanatory functions. The probabilistic demand model that most effectively corrects the bias and random error in the deterministic demand model is developed through this process.

45

As an application, the developed probabilistic demand model is used to construct limit state functions based on specified capacity values and estimate the deformation fragility of an example asymmetric offshore platform. This approach fully considers inherent uncertainties in structural and loading parameters, statistical uncertainties in model parameters, and model errors. Predictive estimates of fragility are used to perform two tasks: (1) Sensitivity analyses of important offshore platform design parameters, and (2) Ultimate limit state and serviceability limit state fragility analyses.

The developed demand model and predictive fragility estimates can give accurate assessments of the reliability of an offshore jacket platform, accounting for all of the prevailing uncertainties. This can be used with a performance based design methodology to increase the overall safety of offshore platforms, while determining the optimal allocation of resources for oil and gas production.

4.2   Future Work

Future research can build upon the reliability analysis presented in this thesis in multiple ways. First, while wave and current actions are usually the dominant environmental loads, there are other more extreme loading conditions, such as seismic loads, blast loads, etc., that can be incorporated into a similar probabilistic demand model. It is not inconceivable that an offshore structure could experience the combined action of these loads; thus, accounting for these other load cases may extend the applicability of the developed probabilistic demand model.

Next, other failure modes in addition to deformation, including shear demand and moment demand, could be considered. This will lead to the formulation of multiple demand models, each constructed in a similar fashion as the deformation demand model presented in this paper. This will make multivariate reliability analyses possible.

Also, the probabilistic demand model developed in this paper gives rise to the necessity of probabilistic capacity models. Capacity models can be formulated in a similar fashion as the formulation of the demand model presented in this paper, as shown by Gardoni et al. (2002). A probabilistic capacity model could be incorporated into the limit state function to conduct reliability analyses that account for prevailing uncertainties in capacity models as well as demand models.

Finally, the reliability framework presented in this paper can be extended to other types of offshore platforms and structures. The formulation of probabilistic models, as outlined in this thesis, is quite general and can be adapted to many offshore engineering applications.

REFERENCES

Bai, J., Gardoni, P., and Hueste, M. B. (2011). "Story-specific demand models and seismic fragility estimates for multi-story buildings." *Structural Safety,* 33(1), 96-107.

Batchelor, G. K. (1967). *Introduction to fluid dynamics.* Cambridge University Press, Cambridge, UK.

Bea, R. G., Xu, T., Stear, J., and Ramons, R. (1999). "Wave forces on decks of offshore platforms." *Journal of Waterway, Port, Coastal, and Ocean Engineering,* 125(3*),* 136-144.

Box, G. E. P., and Cox, D. R. (1964). "An analysis of transformations." *Journal of the Royal Statistical Society. Series B (Methodological),* 26(2), 211-246.

Box, G. E. P., and Tiao, G. C. (1992). *Bayesian inference in statistical analysis.* Wiley, New York, NY.

Chopra, A. K. (2006). *Dynamics of structures: theory and applications to earthquake engineering (3rd ed),* Prentice Hall, Englewood Cliffs, NJ.

Dean, R. G., and Dalrymple, R. A. (1991). *Water wave mechanics for engineers and scientists,* Prentice Hall, Englewood Cliffs, NJ.

Ditlevsen, O., and Madsen, H. O. (1996). *Structural reliability methods,* Wiley, Chichester, UK.

Gardoni, P., Der Kiureghian, A., and Mosalam, K. M. (2002). "Probabilistic capacity models and fragility estimates for reinforced concrete columns based on experimental observations." *Journal of Engineering Mechanics,* 128(10), 1024-1038.

Gardoni, P., Mosalam, K. M., and Der Kiureghian, A. (2003). "Probabilistic seismic demand models and fragility estimates for RC columns." *Journal of Earthquake Engineering,* 7(1), 79-106.

Hahn, G. D. (1992). "Sensitivity of the dynamic response of simple offshore structural models." *Ocean Engineering,* 19(3), 289-301.

Jensen, J. J., Mansour, A. E., and Pedersen, P. T. (1991). "Reliability of jack-up platform against overturning." *Marine Structures,* 4(3), 203-229.

Karamchandani, A., Dalane, J. I., and Bjerager, P. (1991). "Systems reliability of offshore structures including fatigue and extreme wave loading." *Marine Structures,* 4(4), 353-379.

Kirkegaard, P. H., Sorensen, J. D., and Brincker, R. (1991). "Fatigue reliability analysis of a mono tower platform." *Marine Structures,* 4(5), 413-434.

McKay, M. D., Conover, W. J., and Beckham, R. J. (1979). "A comparison of three methods for selecting values of input variables in the analysis of output from a computer code." *Techometrics,* 22(2), 239-245.

Morison, J. R., O'Brien, M. P., Johnson, J. W., and Schaaf, S. A. (1950). "The force exerted by surface waves on piles." *Journal of Petroleum Technology,* 2(5), 149-154.

Nadim, F., and Gudmestad, O. T. (1994). "Reliability of an engineering system under a strong earthquake with application to offshore platform." *Strucutual Safety,* 14(3), 203-217.

Nataraja, R., and Kirk, C. L. (1977). "Dynamic response of a gravity platform under random wave forces." *Proc., Offshore Technology Conference.* Houston, TX.

Ramamoorthy, S. K., Gardoni, P., and Bracci, J. M. (2006). "Probabilistic demand models and fragility curves for reinforced concrete frames." *Journal of Structural Engineering,* 132(10), 1563-1572.

Simpson, T. W., Lin, D. K., and Chen, W. (2001). "Sampling strategies for computer experiments: design and analysis." *International Journal of Reliability and Applications,* 2(3), 209-240.

Skogdalen, J. E., Khorsandi, J., and Vinnem, J. E. (2012). "Evacuation, escape, and rescue experiences from offshore accidents including the Deepwater Horizon." *Journal of Loss Prevention in the Process Industries,* 25(1), 148-158.

Tabatabaei, R. (2011). "Torsional vibration of eccentric building systems." *Recent Advances in Vibrations Analysis*, N. Baddour, ed., InTech.

Xiaoyu, H., and Hongnan, L. (2010). "Torsionally coupled dynamic performance analysis of asymmetric offshore platforms subjected to wave and earthquake loadings." *Earthquake Engineering and Engineering Vibration,* 9(2), 247-259.